

****Volume Title****
ASP Conference Series, Vol. **Volume Number**
****Author****
 © ****Copyright Year**** *Astronomical Society of the Pacific*

Extended atmospheres of AGB stars: modeling and measurement

Michael J. Ireland¹

¹*Sydney Institute for Astronomy (SfA), School of Physics, A28, University of Sydney, NSW 2006, Australia*

Abstract. Encoded in the time- and wavelength dependent properties of pulsating AGB stars are the underlying fundamental parameters of mass, composition and evolutionary state. However, the standard technique of placing stars on a HR diagram, even with the aid of pulsation periods, can not be done easily for extended AGB stars, because of the difficulty of defining a radius or temperature. The atmospheres of Mira variables are so extended that the optical depth unity radius can vary by a factor of 3 over the energetically important region of the spectrum. Many important constituents in the radiative transfer are far from local thermodynamic equilibrium, and for the coolest stars, the process of dust formation and destruction requires a time-dependent model of grain growth. I will describe the challenges and some of the solutions to modeling these atmospheres, and describe the utility of different kinds of observations in helping understand both fundamental parameters and chaotic processes in complex AGB atmospheres.

1. Introduction and Scope

The Asymptotic Giant Branch (AGB) is the evolutionary state where the majority of stars ending their lives today lose the majority of their mass. It is primarily for this reason that they naturally have extended atmospheres, as a photosphere gradually transitions to a stellar wind. AGB stars have much more extended atmospheres than mass-losing hot stars, because winds can only become radiatively driven around AGB stars after dust forms. In turn, this means that an additional mechanism, *pulsation*, is required in order to elevate the material high enough above the photosphere. The resulting picture is rather complex, depending on chemistry, luminosity, evolutionary state, mass, and including effects of time-dependent highly non-linear pulsation, highly supersonic shocks and non-equilibrium dust formation.

It is due to this complexity that the scope of this review must be limited. I will focus on Mira-type variables as the AGB stars with the most extended atmospheres, and will not focus on the super-wind phase. I will spend little time on C-stars both due to personal biases and a lack of as much observational information, and will only consider spherically symmetric properties and models. I will discuss the unique measurements that are possible for pulsating AGB stars in Section 2, , I will discuss the state of modeling efforts and challenges in Section 3, and I will discuss the most important and exciting future goals in Section 4.

2. Unique Measurements

AGB stars have absolute K-magnitudes in the range -6 to brighter than -10, and are the most numerous stars in this magnitude range for all but the very youngest stellar populations. This means that they can be seen to great distances. Their nonlinear pulsation and large angular size means that they can in principle be studied in more detail than arguably any single star other than the sun. In the following sections I will describe a subset of reasons why observations of extended AGB atmospheres are so unique.

2.1. Nearby Details

Within about 500 pc, we can learn a lot about pulsating AGB stars primarily because they can be resolved both spatially and spectrally throughout the energetically important region of their spectra. The smallest Mira variables, with diameters of ~ 1 AU subtend an angular size of 2 mas at 500 pc distances, clearly resolvable on 200 m baselines by both northern and southern hemisphere infrared interferometers.

The early speckle interferometry measurements of Labeyrie et al. (1977) pioneered the study of resolved extended AGB atmospheres, showing that the apparent angular size of the eponymous Mira *o* Ceti varied by a factor of ~ 2 – 3 in and out of TiO absorption features. As will be discussed below, this rather incredible result, when combined with spectra, only makes sense if the dust that is thought to drive the stellar wind is optically thin at all wavelengths, and if the strong TiO features are far from local thermodynamic equilibrium.

Subsequent years have produced many more interferometric results than can be effectively modeled, including: aperture-masking interferometry observations of 10 nearby Miras at $< 1 \mu\text{m}$ wavelengths by Haniff et al. (1995), diameter measurements of 18 nearby Miras at $2.2 \mu\text{m}$ by van Belle et al. (1996), detailed wavelength-dependent (Mennesson et al. 2002; Millan-Gabet et al. 2005; Ireland et al. 2005; Woodruff et al. 2009) and time-dependent diameters (e.g. Woodruff et al. 2008), and the first “true” images of a Mira where the continuum photosphere and shell are well resolved (looking rather spherical after all that hard work) by Le Bouquin et al. (2009). The common observational theme in these measurements is that most, and sometimes all, wavelengths, have a center-to-limb variation with more than one significant component, and that the wavelength-dependence of diameter is more significant than phase- or cycle-dependence. This wavelength-dependence of diameter means that a radius is difficult to define, and consequently, and effective temperature is *not meaningful* in the same way as for compact stars.

A relatively new use of optical interferometry for nearby Miras is to make optical interferometry polarimetry observations, in order to separate scattered light from thermally emitted light. An illustration of how this is possible is given in Figure 1. These observations are particularly important because radiation pressure on dust is thought to be the main driver of AGB stellar winds, and observing the light scattered by dust determines the dust properties and distribution.

This kind of observation was pioneered by Ireland et al. (2005), who demonstrated that dust forms only ~ 2 stellar radii from two Mira variables, R Car and RR Sco, and scatters $\sim 20\%$ of the stellar flux at 900 nm. The SAMPol mode on the CONICA camera at the VLT has extended the availability of this method to the near-infrared at significantly higher signal-to-noise (Norris et al. 2011, in preparation), as shown in Figure 2.

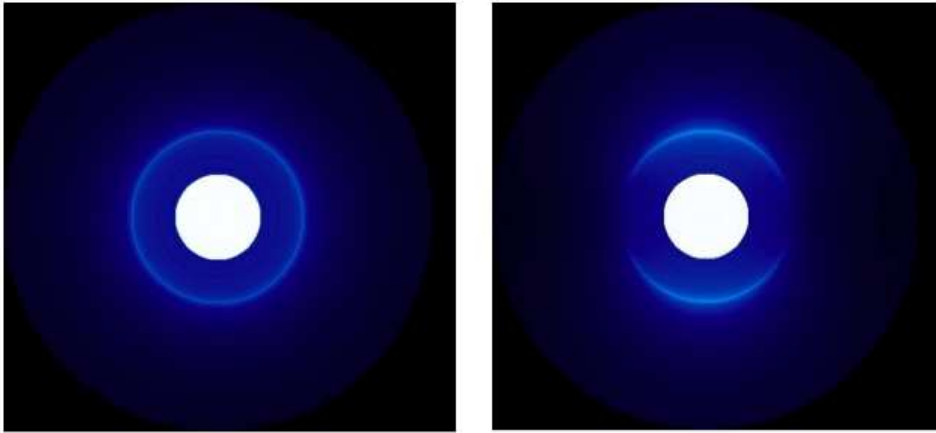


Figure 1. Left: A toy model of a star with dust shell and radiatively-driven wind as seen in unpolarized light. Right: the same model as seen in polarized light with the E-field oriented horizontally. Despite this symmetrical model having zero total polarization, the brightness of the shell as resolved by an interferometer is different depending on if the baseline is parallel or perpendicular to the baseline.

A preliminary result from these multi-wavelength observations is that there is a population of grains at ~ 2 stellar radii that have grain radii of order 300 nm.

In addition to optical and near-infrared interferometry, there are many other unique observations available of nearby Mira variables. Mira variables are some of the only nearby stars that have their continuum photospheres resolvable in the radio (Reid & Menten 1997). These kinds of observations are much easier now with upgrades such as EVLA in the northern hemisphere and CABB in the south. These observations probe the ionization edge of metals such as Na and K in the extended photosphere. Masers in turn probe the velocity structure of the atmosphere (e.g. Cotton et al. 2008).

By virtue of their brightness and appeal to amateur astronomers, nearby Miras also have long photometric time-baselines, up to hundreds of years. This means that period are precise despite the long periods, and long-term period changes (possibly indicating recent thermal pulses) are detectable (e.g. Zijlstra et al. 2002).

Finally, high spectral resolution observations (e.g. Hinkle et al. 1997) have been under-utilized, mainly because of the difficulty in interpretation, and have only been made in select wavelength intervals. These are of course relatively easy observations to make even near minimum-light in the visible, and contain a wealth of information due to the various spectral features that probe different heights in the atmosphere.

2.2. Distant Complexity

For distant Mira variables, particularly those outside the Galaxy, the number of possible observations are much more manageable. Firstly, pulsating AGB stars have all the measurements available for non-pulsating stars, but can be seen to larger distances due to their high luminosities (e.g. Cen A, Rejkuba 2004). This will become even more important with new space missions available for sensitive, deep photometry, especially the JWST (the Virgo cluster, see Section 4). The most important spectral features are broad-band colors, continuum shapes and molecular band strengths - these can all be

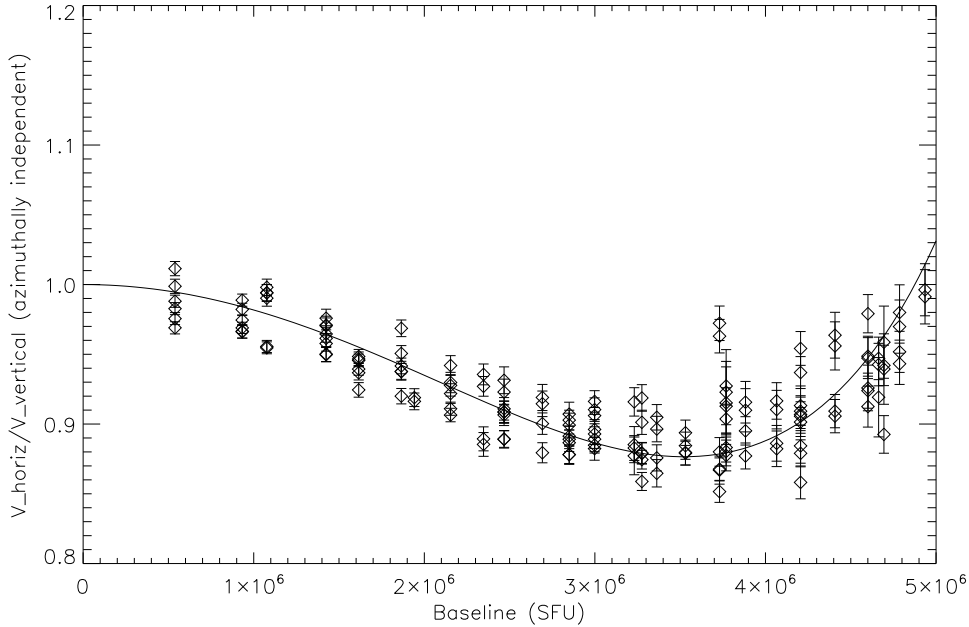


Figure 2. The visibility ratio for polarizations parallel and perpendicular to the interferometric baseline for W Hya at a wavelength of $1.24 \mu\text{m}$ (Norris et al 2011, in preparation). The fit (solid line) is a thin shell model with $\tau_{\text{scat}} \sim 0.1$ and a shell radius of ~ 2 stellar radii.

determined at low spectral resolution so are even easier to observe at large distances than stars of earlier spectral type.

The most important additional observation available for AGB stars is pulsation period. In principle, the combination of the four observationally determined variables of composition (i.e. relative strength of spectral features), temperature, apparent luminosity and period is enough to uniquely determine four fundamental parameters, e.g. composition, distance, luminosity and mass. Of course, correct interpretation is dependent on identifying the correct pulsation mode, and having trustworthy models! In addition, AGB stars may have more hidden variables, such as core mass (which does not uniquely determine luminosity in the presence of thermal pulses) and reddenning law.

Going one step further, the large amplitude pulsation that produces the extended AGB atmospheres means that nonlinear phenomena are constrained by observations of pulsation amplitude and light-curve shape. These observations are necessarily made whenever a period is measured. This information has been used in the case of Cepheid variables in the Large Magellanic Cloud (LMC) by Keller & Wood (2006) to uniquely constrain all fundamental parameters including the distance to the LMC. For the case of Mira variables, however, period-luminosity-color relationships have been used successfully (Feast et al. 1989), but period-luminosity-color-amplitude or more complex relationships have not. Calibration of such relationships and a quantitative understanding of the width of the Mira period-luminosity relationship are needed before these observations of distant AGB stars can be used optimally.

3. Modeling Challenges

Making comprehensive models of pulsating AGB stars is the only way to understand underlying physical parameters of initial mass, composition and evolutionary state. There is some hope to calibrate models indirectly, e.g. statistical initial masses of a population using kinematics Wyatt & Cahn (e.g. 1983), initial composition of cluster Miras or confirming that the same models work for low-amplitude cluster Miras (e.g. Lebzelter & Wood 2007) or possibly smaller-amplitude AGB variables in binary stars. Masses of individual Mira variables are not likely to be measured from binary orbits due to the very long periods involved. Even for Mira itself, a relatively wide binary with a ~ 1000 year period, wind accretion phenomena onto the secondary and pulsation in the primary would complicate obtaining a spectroscopic orbit even if the time baseline were available.

Specialized model atmospheres are needed for Mira variables because the atmospheric extension is so important in interpreting spectra and other observations. For example, water shells are observed at radii of ~ 2 times the continuum photospheric radius (e.g. Le Bouquin et al. 2009). This means that the geometrical dilution of the radiation field at the location of this shell gives a factor of ~ 4 times less flux as compared to an equivalent shell located just above the continuum photosphere, and means that the temperature of this layer is $\sim 30\%$ cooler than it would be in a compact model. This extension can not be produced by a static model, so the run of density with radius must come from a dynamical pulsation code. The radiative transfer calculation therefore involves a spherical atmosphere that is poorly approximated by the plane-parallel case (e.g. Figure 3). Although many static model codes (e.g. MARCS, Gustafsson et al. 2008) are spherical, they have not generally been used to model atmospheric structures as extreme as Mira variables, and do not have an easy way to interface with dynamical codes.

Several groups have produced competitive dynamical, extended atmosphere codes for modeling AGB stars. Codes that are currently in use are the Cool Opacity-sampling Dynamic EXtended (CODEX) models by the Sydney-Canberra-Heidelberg group (Ireland et al. 2008), and the Uppsala code (e.g. Höfner et al. 2003). The CODEX models have only been used to model M-type Miras, while the Uppsala code has been mostly used for C-type Miras, but has more recently been applied to S- and M-type Miras also. Woitke (2006) and Jeong et al. (2003) described codes that had relatively simple radiative transfer but sophisticated O-rich grain growth descriptions. To the author's knowledge, these codes are not in active use today.

Some of the key differences between the two codes in active use are given in Table 1. At the time of writing, there are various compromises made in each case. The CODEX models are a marriage between detailed gray self-excited pulsation models (e.g. Keller & Wood 2006) and an opacity-sampling code that re-solves for temperature in the outer atmosphere at selected model phases, based on the method of Schmid-Burgk & Scholz (1984). This outer atmosphere code uses an opacity sampling method and dust formation approximations only expected to be valid within a few continuum-forming radii, where grain growth time-scales are small compared to the pulsation time-scale (Ireland & Scholz 2006). The Uppsala models simultaneously combine dynamics and radiative transfer into a single large implicit difference equation scheme which is solved with Newton-Raphson iteration. These models include the time-dependent growth of a single grain species, but has the capability for much more sophisticated heterogeneous grain growth in the code (Höfner 2010, personal commu-

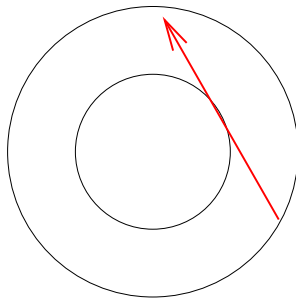
nication). The Uppsala code introduces pulsation with a sinusoidal piston at the base of the atmosphere, which means that detailed phase-dependent results may not be reliable and that it is more difficult to relate model properties to fundamental parameters. Although the CODEX models are self-excited, there are two key free parameters in the models that have not been calibrated, so their ability to relate model properties like pulsation amplitude to underlying physical parameters is an in-principle strength only.

Table 1. A comparison of key model properties of the two actively used dynamical extended atmosphere codes.

Model Property	CODEX	Uppsala
Pulsation	Self-Excited	Piston
Pressure Structure	From Gray Model	Self-Consistent
Temperature Structure	Opacity-Sampling (4300 wavelengths)	Opacity-Sampling (64 to 300 wavelengths)
Dust Condensation	Modified chemical equilibrium	Time-dependent nucleation and grain growth
Molecular non-LTE	Optional Extension	Not included
Dust Scattering	Isotropic	Isotropic

Qualitatively, the model structures of dynamical codes appear periodic in the lower atmosphere ($\tau_c \sim 1$) but chaotic in the upper atmosphere, as seen in Figure 4. Where models include a wind, the transition to the radiatively driven wind region occurs at $\sim 2\text{--}5$ continuum-forming radii (e.g Fig. 2 of Höfner et al. 2003). Even in the deepest layers, the motion is not sinusoidal due to the strong non-linear effects (most importantly, shocks) that damp the pulsations.

The majority of observed properties of pulsating, extended AGB stars, including wavelength-dependent interferometric diameters (Woodruff et al. 2009), low- and high-resolution spectra, light curve shapes and phase-lags between wavelengths (Ireland et al, 2011, submitted) can all be reproduced to some extent by the modern codes in certain instances. A few key model properties and challenges will be presented below, focusing on the CODEX models which the author is most familiar with.



Spherical Codes must include rays that go inwards then outwards to model shells correctly.

Figure 3. The kind of ray that is key to solving for radiative equilibrium in an extended spherical code. For purposes of computational efficiency, different spherical codes use different number of these rays or other approximations, and may not be suited to the very extended configurations in Mira variables.

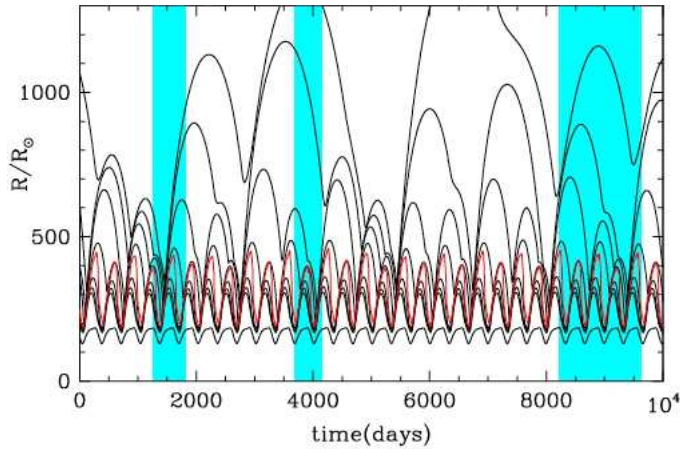


Figure 4. An example model structure used in Ireland et al. (2008) for the o54 series, showing the position of the mass zones as a function of time. The layers around the photosphere ($\sim 250 R_{\odot}$) have a periodic motion, while the outer layers show chaotic motions. [Electronic version only: The red lines show the position of the optical-depth $2/3$ layer and the blue shaded regions show the cycles chosen for detailed radiative transfer modeling.]

3.1. Molecular Shells

Very extended dust shells have been seen around AGB stars for decades (e.g. Danchi et al. 1994) but only in the past decade has it been clear that molecular shells, particularly H_2O shells, exist around Mira variables (e.g. Mennesson et al. 2002). Published models have naturally explained these water “shells” ever since they were observed (Tej et al. 2003) with a monotonic decrease in gas density with increasing radius, coupled with a sharp increase in H_2O condensation fraction as the temperature decreases with radius. These molecular shells may therefore be quite different from shells produced where radiative acceleration of dust becomes important, which can cause increases of density with radius at the base of a shell being driven away radiatively (e.g. Höfner et al. 2003).

3.2. Mass Loss and Radiation Pressure

The details of the mass-loss process in extended AGB stars is the subject of much active research and debate (e.g. Woitke 2006; Höfner 2008). Even simple questions, like “*can pulsation alone drive measurable mass loss?*” have not been clearly answered in the literature, as no self-excited code has the mass resolution to resolve mass loss rates smaller than $10^{-7} M_{\odot} \text{ yr}^{-1}$. However, it is generally accepted that only a combination of pulsation and radiative acceleration can cause the significant mass loss rates of $> 10^{-7} M_{\odot} \text{ yr}^{-1}$ seen in “typical” M-type Miras.

Neglecting scattering and assuming full dust condensation in chemical equilibrium, when L/M (luminosity/mass in solar units) exceeds $\sim 3,000(0.02/Z)$ (O-rich) or $\sim 300(0.02/Z)$ (C-rich, $C/O=2$), radiation can drive winds. For C-rich stars, the relatively high condensation temperature of carbon dust means that the material does not have to be elevated very far above the photosphere for enough dust to condense to

drive a wind. The difficulty in modelling effective mass loss in O-rich stars is elevating enough material to radii of $\sim 5\text{--}10$ continuum-forming radii, where Fe-rich silicates can fully condense.

An intriguing method of driving winds was recently given in Höfner (2008), by scattering from grains of several hundred nm radius. Both the relatively small angular sizes measured in-between TiO absorption bands in visible/near-IR interferometry and optical interferometric polarimetry observations demonstrate that any scattering must be optically-thin (Section 2.1). However, it is still possible to drive a wind with only a small optical depth in scattering, as long as the shell mass is small.

The most direct observational constraint on the capability for dust scattering to drive winds is to simultaneously consider a tracer of gas mass and a tracer of dust scattering optical depth. At moderate or low spectral resolution, the shell mass is best probed with interferometric observations in the near infrared (1.2 through to 4 microns) that measure the H₂O optical depth and enable the shell mass to be inferred.

To date there is no paper clearly combining column density constraints of H₂O and dust scattering. What has been done is to compare dynamical models of Mira variables to observations in the near-infrared (Woodruff et al. 2009) and to independently compare these models to diameter measurements at wavelengths $< 1\ \mu\text{m}$ where scattering dominates (Ireland & Scholz 2006; Ireland et al. 2008). The models are only able to simultaneously reproduce the extension at wavelengths sensitive to H₂O and the smaller diameters in-between TiO bands at e.g. 830 nm if the grain radius of silicate grains is less than approximately 70 nm.

3.3. Non-LTE in Extended Atmospheres

For the strong electronic transitions of TiO that define the M-type spectral sequence, typical Einstein A coefficients are $\sim 10^7$ Hz. This is much higher than collision rates which are $< 10^3$ Hz in the TiO forming layers for $\log(g) < 0$. Despite this, static models reproduce TiO bands reasonably well (e.g. Plez 1998). For very extended dynamical models, however, the Local Thermodynamic Equilibrium (LTE) assumption reproduces observed band depths poorly. The reason for this can be seen in Figure 5, where the lower temperatures in the outer layers of the dynamic model causes much deeper than observed bands. This kind of temperature difference makes a factor of ~ 100 difference in the Planck function in e.g. the deep TiO absorption feature at 670 nm. As no features have depths of more than a factor of a few relative to the neighboring pseudo-continuum, non-LTE effects play a very significant role in the $\sim 450\text{--}900$ nm region of M-type Mira spectra. A code that includes these non-LTE effects is therefore essential if model comparisons to visible light curves or spectral types are to be made.

At the time of writing, no extended code yet solves for the level populations of molecules self-consistently. The approximation used in the CODEX models is a fluorescence scattering approximation, where the rovibrational states and the relative population in the ground singlet and ground triplet state are in LTE, but transitions to and from the excited electronic states are modeled as a scattering process with appropriate wavelength redistribution. Details of this method are given in Ireland et al. (2008). As the existing database of visible light curves and visible spectral types is so rich, it is essential that in time models can make reliable predictions in the visible wavelength range.

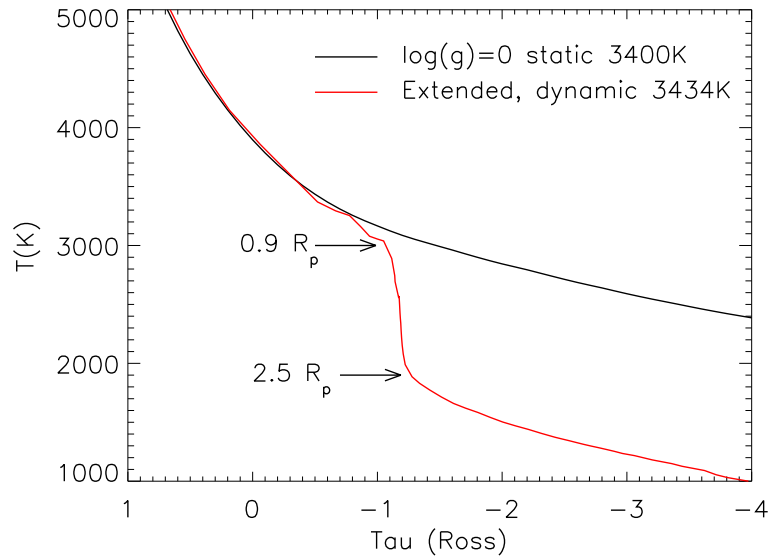


Figure 5. The comparison of a static and dynamic LTE model atmosphere temperature profile with similar $\log(g)$ and effective temperature. The dilution of the radiation field due to geometrical extension causes the temperature to be very much reduced at small optical depths. R_p is the “parent-star” static model radius.

4. Summary and Brave Future Goals

It is clear that the wealth of observations already available of extended AGB stars can not be accurately modeled. The state of observational knowledge 33 years ago included visible light curves, the pioneering multi-wavelength interferometry of Labeyrie et al. (1977) and spectral types in the visible. No current modeling effort to date can reproduce these observations and give insight into the underlying parameters of the prototypical Mira variable *o* Ceti. However, much progress has been made, with current models qualitatively reproducing all the observed features and the only matter of serious debate being the dominant factors in pulsating AGB star mass-loss and the best parameter choices for modeling convection.

In the next decade, imaging extended atmospheres will become routine, and with polarimetric measurements, dust shells will be resolved as a function of pulsation phase for a number of nearby typical Miras. But more important than these nearby details will be the contribution of time-domain astronomy with the world’s largest telescopes.

In the Virgo cluster, individual Miras have apparent K-magnitudes of ~ 23 and individual Miras in the Coma cluster will have K-magnitudes of ~ 27 . These magnitudes are within reach of JWST or large ground-based Extremely Large Telescopes. For the ellipticals in Virgo in particular, these Miras could be a superb tool for extragalactic archaeology: determining the star-formation history and indirectly the merger history of distant galaxies. This will be possible because such a wealth of information (broad-band colors including colors sensitive to molecular band depths, period, amplitude) will be available for no other single star in an old stellar population. With this information, the fundamental parameters of composition, initial mass and evolutionary state will be able to be derived for a great number of Miras.

Of course, none of this will be possible unless our understanding of extended AGB star atmospheres is first tested and calibrated against nearby Mira prototypes. We need to establish that our treatment of convection in self-excited pulsation is adequate and have an calibrated prescription for the free parameters, and we need to come to an understanding and consensus on the most important parts of a dust formation model that can drive stellar winds. In the author's opinion, these challenges are not insurmountable, and significant progress will be made prior to the next *Why Galaxies Care* conference.

Acknowledgments. The Author would like to thank B. Norris for making the polarimetric reduction of W Hya available in advance of publication, and would like to thank M. Scholz for helpful discussions. M. Ireland is supported by an Australian Research Council Postdoctoral Fellowship (project number DP0878674).

References

- Cotton, W. D., Perrin, G., & Lopez, B. 2008, *A&A*, 477, 853
- Danchi, W. C., Bester, M., Degiacomi, C. G., Greenhill, L. J., & Townes, C. H. 1994, *AJ*, 107, 1469
- Feast, M. W., Glass, I. S., Whitelock, P. A., & Catchpole, R. M. 1989, *MNRAS*, 241, 375
- Gustafsson, B., Edvardsson, B., Eriksson, K., Jørgensen, U. G., Nordlund, Å., & Plez, B. 2008, *A&A*, 486, 951. [0805.0554](#)
- Haniff, C. A., Scholz, M., & Tuthill, P. G. 1995, *MNRAS*, 276, 640
- Hinkle, K. H., Lebzelter, T., & Scharlach, W. W. G. 1997, *AJ*, 114, 2686
- Höfner, S. 2008, *A&A*, 491, L1
- Höfner, S., Gautschy-Loidl, R., Aringer, B., & Jørgensen, U. G. 2003, *A&A*, 399, 589
- Ireland, M. J., & Scholz, M. 2006, *MNRAS*, 367, 1585. [astro-ph/0601383](#)
- Ireland, M. J., Scholz, M., & Wood, P. R. 2008, *MNRAS*, 391, 1994
- Ireland, M. J., Tuthill, P. G., Davis, J., & Tango, W. 2005, *MNRAS*, 361, 337
- Jeong, K. S., Winters, J. M., Le Bertre, T., & Sedlmayr, E. 2003, *A&A*, 407, 191
- Keller, S. C., & Wood, P. R. 2006, *ApJ*, 642, 834. [astro-ph/0601225](#)
- Labeyrie, A., Koechlin, L., Bonneau, D., Blazit, A., & Foy, R. 1977, *ApJ*, 218, L75
- Le Bouquin, J., Lacour, S., Renard, S., Thiébaud, E., Merand, A., & Verhoelst, T. 2009, *A&A*, 496, L1. [0902.3698](#)
- Lebzelter, T., & Wood, P. R. 2007, *A&A*, 475, 643. [0710.0953](#)
- Mennesson, B., Perrin, G., Chagnon, G., du Coudé Foresto, V., Ridgway, S., Merand, A., Salome, P., Borde, P., Cotton, W., Morel, S., Kervella, P., Traub, W., & Lacasse, M. 2002, *ApJ*, 579, 446
- Millan-Gabet, R., Pedretti, E., Monnier, J. D., Schloerb, F. P., Traub, W. A., Carleton, N. P., Lacasse, M. G., & Segransan, D. 2005, *ApJ*, 620, 961. [arXiv:astro-ph/0411073](#)
- Plez, B. 1998, *A&A*, 337, 495
- Reid, M. J., & Menten, K. M. 1997, *ApJ*, 476, 327
- Rejkuba, M. 2004, *A&A*, 413, 903
- Schmid-Burgk, J., & Scholz, M. 1984, *Transfer in spherical media using integral equations (Methods in Radiative Transfer, Kalkofen W. Ed.)*, 381
- Tej, A., Lançon, A., & Scholz, M. 2003, *A&A*, 401, 347
- van Belle, G. T., Dyck, H. M., Benson, J. A., & Lacasse, M. G. 1996, *AJ*, 112, 2147
- Woitke, P. 2006, *A&A*, 452, 537. [astro-ph/0602371](#)
- Woodruff, H. C., Ireland, M. J., Tuthill, P. G., Monnier, J. D., Bedding, T. R., Danchi, W. C., Scholz, M., Townes, C. H., & Wood, P. R. 2009, *ApJ*, 691, 1328. [0811.1642](#)
- Woodruff, H. C., Tuthill, P. G., Monnier, J. D., Ireland, M. J., Bedding, T. R., Lacour, S., Danchi, W. C., & Scholz, M. 2008, *ApJ*, 673, 418. [arXiv:0709.3878](#)
- Wyatt, S. P., & Cahn, J. H. 1983, *ApJ*, 275, 225
- Zijlstra, A. A., Bedding, T. R., & Mattei, J. A. 2002, *MNRAS*, 334, 498